CFD Modelling of Transient Thermo-Fluid Dynamics in Liquid Hydrogen Storage

Daniele Melideo[a], Silvia Melani[a], Sara Evangelisti[b], Lorenzo Ferrari[a]

[a] Dipartimento di Ingegneria dell'Energia, dei Sistemi, del Territorio e delle Costruzioni (DESTEC), Università di Pisa, Largo Lucio Lazzarino - 56122 Pisa – Italy, daniele.melideo@unipi.it
[b] Gas and Heat S.p.A., Via Livornese, 796 - 56122 Pisa – Italy

Abstract

The growing interest in liquid hydrogen (LH_2) as an energy carrier for maritime transport calls for reliable predictive tools capable of describing the complex fluid dynamic phenomena occurring inside cryogenic storage tanks under ship-motion-induced excitations. Among these phenomena, sloshing plays a key role, as it may generate significant free-surface oscillations, transient pressure loads on tank walls, and enhanced internal fluid motion, with possible implications for both structural design and thermo-fluid behaviour.
In this work, a Computational Fluid Dynamics (CFD) model is developed to investigate the sloshing dynamics of LH_2 in a partially filled storage tank under oscillatory conditions representative of marine applications. The study focuses on the hydrodynamic response of the liquid to external forcing, with particular attention to free-surface evolution, resonance-related effects, and the influence of excitation frequency and filling level on the overall tank behaviour. A preliminary theoretical framework based on linear wave theory is used to estimate the natural sloshing frequency and to identify the most critical excitation conditions.
The numerical activity is intended to provide a first step toward the characterization of LH_2 tank behaviour under dynamic operating conditions, establishing a basis for future extensions toward coupled thermo-fluid analyses, including thermal stratification, phase change, and boil-off phenomena. The results contribute to the development of modelling tools to support the design and safety assessment of liquid hydrogen storage systems for next-generation maritime energy applications.

Keywords:

Liquid hydrogen; Sloshing; CFD modelling; Cryogenic storage; Maritime transport; Free-surface dynamics.

1. Introduction

The ongoing energy transition, driven by the need to reduce greenhouse gas emissions and comply with long-term climate targets, is accelerating the deployment of renewable energy sources and reshaping the structure of energy systems worldwide. In this context, the increasing penetration of wind and solar power, while essential for decarbonization, also introduces major challenges related to intermittency, temporal mismatch between supply and demand, and the need for large-scale energy storage and system flexibility. Therefore, there is growing interest in energy carriers capable of storing energy over medium and long timescales and enabling the integration of renewable electricity into sectors that are difficult to electrify directly. Hydrogen is widely regarded as one of the most promising options in this framework [1].
Hydrogen is not a primary energy source, since it is not freely available in nature and must be produced from other resources using fossil, nuclear, or renewable energy. Its importance lies in its role as an energy vector, namely a substance able to store, transport, and release energy generated elsewhere. This makes hydrogen particularly attractive in future low-carbon energy systems, where surplus electricity from renewable sources can be converted into hydrogen through water electrolysis and later reused for power generation, mobility, industrial processes, or synthetic fuel production. In this sense, hydrogen is not only a fuel, but also an enabling technology for sector coupling and long-duration storage [2–5].
The relevance of hydrogen is especially pronounced in hard-to-abate sectors, where direct electrification is limited by operational, volumetric, or weight constraints. Maritime transport is one of the most representative examples. Shipping requires energy carriers with high gravimetric energy density, acceptable volumetric compactness, and suitability for long-range operation. Conventional fossil fuels still dominate this sector, but the decarbonization pressure is rapidly increasing. In this scenario, hydrogen-based fuels are emerging as potential alternatives for low- or zero-carbon propulsion. Among the available storage options, liquid hydrogen

(LH_2) is particularly interesting because it offers a much higher volumetric energy density than gaseous hydrogen, making it more suitable for onboard storage where tank volume is a critical issue. This is one of the reasons LH_2 is increasingly considered for heavy-duty, maritime, and aerospace applications [6].

At the same time, the adoption of LH_2 is far from straightforward. Although hydrogen has the highest gravimetric energy content among common fuels, with a lower heating value of about 120 MJ/kg and a higher heating value of about 144 MJ/kg, its volumetric energy density at ambient conditions is extremely low. As a result, hydrogen must be either compressed, liquefied, or stored in alternative carriers or materials to become practical for transport applications. Liquefaction strongly reduces the storage volume, but it also requires cryogenic temperatures close to 20 K, leading to significant energy consumption and complex thermal management requirements. Moreover, hydrogen presents several safety-related challenges, including wide flammability limits, low ignition energy, high diffusivity, and possible material degradation phenomena such as hydrogen embrittlement [7].

From a thermodynamic viewpoint, LH_2 storage is particularly demanding. Hydrogen has a critical temperature of about 33.1 K, a normal boiling point of about 20.3 K at atmospheric pressure, and a triple point at 13.8 K and 7.2 kPa. These characteristic values highlight how narrow the liquid region is and how sensitive the fluid is to even modest heat ingress from the environment. In practical systems, complete thermal isolation is impossible, and therefore some degree of evaporation is unavoidable. This leads to boil-off, internal pressure rise, and the need for appropriate pressure management strategies. The issue is even more critical in liquid hydrogen than in LNG systems, because LH_2 has a very low enthalpy of vaporization, around 0.45 kJ/g, which makes it highly susceptible to phase change even under relatively small thermal loads. The resulting boil-off gas may be vented, re-liquefied, or reused, but in all cases, it affects system efficiency, safety, and operational planning [8].

These challenges become even more complex in maritime applications, where cryogenic tanks are exposed not only to thermal loads but also to dynamic excitations associated with ship motion. In partially filled tanks, vessel roll and pitch can induce oscillatory motion of the liquid free surface, commonly referred to as sloshing. This phenomenon has long been recognized as a key design issue in marine engineering because it generates time-dependent hydrodynamic forces and moments, modifies wall pressure distributions, and may produce severe local impact loads under near-resonant conditions. In cryogenic hydrogen tanks, however, sloshing is not merely a structural concern. The motion of the liquid can also influence the liquid-vapor interface, enhance internal mixing, alter temperature stratification, and potentially intensify heat and mass transfer processes related to evaporation. Therefore, in LH_2 storage systems, sloshing should be regarded as a coupled hydrodynamic and thermodynamic phenomenon rather than as a purely mechanical one [9].

Although sloshing has been extensively studied for conventional fluids and, to some extent, for LNG tanks, the available literature on LH_2 tanks remains comparatively limited, especially when the interaction between internal fluid motion and thermodynamic response is considered. Existing studies indicate that the intensity of sloshing depends strongly on tank geometry, filling level, excitation amplitude and frequency, and proximity to the natural sloshing modes of the liquid. In marine conditions, this is particularly relevant because the characteristic pitch period of the vessel may become comparable to the first natural sloshing period of the contained fluid, leading to dynamic amplification. For this reason, the hydrodynamic characterization of sloshing is a necessary step toward the development of more advanced predictive models for LH_2 storage onboard ships [10].

Within this framework, the present work focuses on the CFD modelling of sloshing in liquid hydrogen storage tanks for maritime transport applications. The objective is to investigate the free-surface dynamics of LH_2 under oscillatory excitation representative of ship motion, and to provide a robust basis for the future analysis of coupled phenomena such as thermal stratification, pressure evolution, and boil-off. By addressing sloshing as a key transient process in marine LH_2 storage, the study contributes to the broader development of numerical tools for the safe and efficient design of next-generation hydrogen-based propulsion and storage systems

2. Hydrogen Properties and Storage Pathways for Maritime Applications

Hydrogen is widely regarded as a strategic energy carrier for future low-carbon energy systems because it can store energy produced from renewable, nuclear, or fossil primary sources and release it in multiple end-use sectors. Its main advantage lies in its exceptionally high gravimetric energy density, which is higher than that of conventional fuels. The lower heating value of hydrogen is approximately 120 MJ/kg, while the higher heating value is about 144 MJ/kg. This makes hydrogen particularly attractive for applications in which mass is a critical design constraint, such as heavy-duty transport, maritime systems, and aerospace applications. However, this important advantage is counterbalanced by its very low volumetric energy density under ambient conditions. As a result, hydrogen cannot be efficiently stored or transported in large quantities unless its density is significantly increased through compression, liquefaction, or alternative storage pathways [11,12].

From a thermo-physical standpoint, hydrogen also presents several distinctive features that strongly influence storage system design. It is the lightest element, highly diffusive, colorless, odorless, and non-toxic, but it also exhibits a wide flammability range in air and a very low ignition energy, which raises relevant safety concerns in case of leakage. The flame is nearly invisible and characterized by low thermal radiation, which makes accidental fires more difficult to detect. In addition, hydrogen can induce material degradation phenomena such as hydrogen embrittlement in metals and blistering in polymers, owing to its small molecular size and high diffusivity. Another important peculiarity is the Joule-Thomson behavior: unlike many common gases, hydrogen may warm upon expansion over part of its operating range, which must be considered when analyzing depressurization or release processes [13] .

The thermodynamic region where hydrogen can exist in liquid form is also very narrow. Hydrogen has a critical temperature of 33.145 K, a critical pressure of 1.3 MPa, a normal boiling point of about 20.3 K at atmospheric pressure, and a triple point at 13.8 K and 7.2 kPa. These values explain why liquefaction is technologically demanding and why even small external heat inputs can produce phase change. For moderate pressures, hydrogen density can be approximated with the ideal gas law, but at higher pressures more accurate equations of state, such as Redlich-Kwong or Peng-Robinson, are required to reproduce real-gas behavior. This aspect is relevant whenever compressed or cryo-compressed storage conditions are considered [14].

Another key aspect for cryogenic storage is the existence of different molecular spin isomers, namely ortho-hydrogen and para-hydrogen. At room temperature, normal hydrogen is a mixture containing about 75% ortho-hydrogen and 25% para-hydrogen, whereas liquid hydrogen at 20 K is composed almost entirely of para-hydrogen, approximately 99.8%. The ortho-to-para conversion is accompanied by heat release, and therefore the liquefaction process must include the removal of this conversion heat. This phenomenon has direct implications for storage behavior. In cryo-compressed systems, part of the environmental heat input can be absorbed by the reverse para-to-ortho conversion rather than being used entirely for liquid evaporation. In contrast, in conventional liquid hydrogen tanks, environmental heat leakage directly promotes evaporation and thus boil-off [15,16].

The conventional hydrogen storage technologies can be grouped into three main categories: compressed gaseous hydrogen, liquid hydrogen, and cryo-compressed hydrogen. Compressed hydrogen storage relies on high-pressure tanks, typically in the range of 250 to 700 bar. This approach is technologically mature and avoids cryogenic conditions, but it suffers from low volumetric efficiency and requires massive pressure vessels, which penalize both storage density and system weight. The gravimetric storage efficiency of compressed-gas systems may be very low, around 5%, meaning that the tank mass can be much larger than the stored hydrogen mass [17–21].

Cryo-compressed hydrogen combines very low temperatures with elevated pressures, typically by storing hydrogen near liquid-hydrogen temperatures but at pressures of the order of 250-350 bar. In principle, this solution increases density beyond standard compressed gas storage, but it also combines the penalties of both cooling and compression. For this reason, it is often considered less attractive in practice for many applications, unless a specific system-level advantage justifies the added complexity. Nevertheless, cryo-compressed storage can partially benefit from the thermodynamic effect of ortho-para conversion, which may mitigate evaporation relative to conventional LH_2 tanks [22].

Among conventional solutions, liquid hydrogen is particularly attractive when storage volume is a major constraint. LH_2 is typically stored in cryogenic tanks at temperatures close to 20 K and at relatively low pressures, generally up to about 10 bar. Compared with gaseous hydrogen, liquefaction leads to a much higher volumetric energy density and drastically reduces the required storage volume. The thesis reports that the liquid-to-gas volumetric ratio is approximately 1:848, which clearly illustrates the benefit of liquefaction for long-range transport applications. This is precisely the reason LH_2 is increasingly considered for heavy-duty transport, maritime shipping, and aerospace systems, where compact storage is essential.

At the same time, LH_2 is also the most thermally sensitive among the conventional storage options. Even with highly insulated cryogenic tanks, complete thermal isolation is impossible, and some heat ingress from the environment is unavoidable. Because hydrogen has a very low boiling point and a low enthalpy of vaporization, about 0.45 kJ/g, even relatively small heat fluxes may trigger evaporation and produce tank self-pressurization. The latent heat of vaporization is reported to be about 18 times lower than that of LNG, which means that LH_2 is considerably more sensitive to heat leakage than liquefied natural gas. This feature is one of the main engineering drawbacks of LH_2 storage and one of the key reasons why accurate thermo-fluid modelling is needed.

The vapor generated by heat ingress is commonly referred to as boil-off hydrogen. If the pressure rises beyond allowable limits, the excess gas must be managed through controlled venting, recovery, re-liquefaction, or direct use in auxiliary systems such as fuel cells. The thesis reports a typical hydrogen loss due to venting on the order of 1-5% per day, which represents a major energetic and economic penalty. For this reason, boil-off is one of the main limitations of LH_2 as an energy carrier. This is especially relevant in large-scale or onboard applications, where the interaction between internal flow motion, thermal stratification, and phase change may further intensify pressure evolution.

Beyond the three conventional approaches, several alternative or emerging hydrogen storage options have been proposed. These include underground storage in caverns or depleted reservoirs, hydrogen carriers such

as ammonia and synthetic fuels, blending with natural gas, metal hydrides, nanostructured carbon materials, and physical adsorption in porous materials such as activated carbons or metal-organic frameworks. These options may offer advantages in terms of storage density, transport logistics, or operating pressure, but they also involve additional penalties related to conversion efficiency, complexity, toxicity, purity constraints, or material cost. Therefore, despite the growing interest in these alternatives, liquid hydrogen remains one of the most relevant solutions whenever high storage density and direct hydrogen use are required.

3. Sloshing Phenomenon

Sloshing is the oscillatory motion of a liquid free surface inside a partially filled tank subjected to external excitation. This phenomenon produces time-dependent pressure distributions on the tank walls, leading to hydrodynamic forces and moments that may affect the structural response of the containment system. The intensity of sloshing depends on the tank geometry, fill level, fluid properties, and excitation characteristics.
When the excitation frequency approaches one of the natural frequencies of the liquid, resonance effects may occur, leading to significant amplification of the free-surface motion. Under such conditions, large wave elevations, impact pressures, and even wave breaking may develop. These effects are particularly relevant in transport applications, where the imposed motion may persist over long periods.
In the case of cryogenic liquids such as LH_2, sloshing is not only a structural issue. The internal motion may increase liquid-vapor interfacial area, promote mixing, and affect heat and mass transfer inside the tank. As a consequence, sloshing may influence pressure evolution and evaporation dynamics, thereby contributing indirectly to boil-off. This is one of the reasons why sloshing deserves special attention in liquid hydrogen storage systems for marine use.
From a modelling perspective, sloshing can be analyzed with different levels of complexity. For small-amplitude motions, linear potential-flow theory can be used to estimate natural frequencies and mode shapes. For larger motions, however, nonlinear effects become important and numerical tools such as CFD are needed to capture the free-surface evolution, pressure fields, and dissipation mechanisms with sufficient accuracy.
In the present context, the relevance of sloshing is further enhanced by maritime application. Pitch and roll motions of the vessel act as dynamic forcing terms, and the first natural sloshing mode may be strongly excited if the corresponding frequencies are close. This makes the analysis of sloshing modes and excitation conditions essential for the design and operation of onboard LH_2 tanks.

3.1. Linear Wave Theory (Airy Theory)

The simplest theoretical framework for describing free-surface wave motion is the linear wave theory, also known as Airy theory. This approach assumes that the fluid is incompressible and inviscid, that the flow is irrotational, and that the free-surface oscillations are small compared with the characteristic dimensions of the domain. Under these assumptions, the governing equations can be linearized and analytical expressions for wave motion can be derived.

$$\eta(x,t) = asin(kx - \omega t) \qquad \textit{Equation 1}$$

where a is the wave amplitude, $k$is the wave number, and ω is the angular frequency [10] [23]. The relation between frequency and wavelength is given by the dispersion relation:

$$\omega_2 = \sqrt{gktanh(kh)} \qquad \textit{Equation 2}$$

where g is the gravitational acceleration and h is the liquid depth. This equation shows that wave dynamics depend on both gravity and fill height
In a partially filled tank, sloshing can be interpreted as a confined gravity-wave problem. The natural sloshing modes correspond to standing waves that satisfy the geometric constraints of the tank. The first mode is usually the most relevant in practice because it is the easiest to excite during ship motion. In a horizontal cylindrical tank with end caps, the characteristic dimension controlling the longitudinal sloshing mode is mainly the effective cylindrical length rather than the total tank length.
Airy theory is useful because it provides a first estimate of natural frequencies and resonance conditions, which are essential for setting up experiments and CFD simulations. However, its validity is limited to small-amplitude oscillations. When wave steepness increases, or when breaking, impact, and strong nonlinearities occur, more advanced numerical approaches are required.

3.2. Liquid Sloshing dynamics

Liquid sloshing is the oscillatory motion of the free surface in a partially filled tank subjected to external excitation. This motion generates time-dependent pressure distributions on the tank walls, leading to hydrodynamic forces and moments that can significantly affect the dynamic response of the containment

system. The intensity of sloshing depends on several parameters, including tank geometry, filling level, fluid properties, and the amplitude and frequency of the imposed motion. In practical applications, sloshing is of major importance in marine, automotive, aerospace, and cryogenic storage systems, where the fluid motion may affect both structural integrity and operational safety.
When the forcing frequency approaches one of the natural frequencies of the liquid, resonance effects may occur, resulting in a significant amplification of free-surface oscillations. Under these conditions, the liquid may produce large distributed hydrodynamic loads, or, in more severe cases, localized impact pressures associated with violent free-surface motion and wave breaking. For this reason, resonance is generally regarded as one of the most critical conditions in sloshing analysis. In cryogenic tanks, the relevance of this phenomenon is even greater, since fluid motion may also affect liquid-vapor interaction, thermal stratification, and evaporation processes.
From a modelling perspective, sloshing may be studied in either the linear or the nonlinear regime. In the linear regime, valid for small free-surface oscillations compared with the tank dimensions, the fluid is commonly assumed incompressible, inviscid, and irrotational, and the problem can be treated through velocity-potential theory. This framework allows the analytical determination of natural frequencies and modal shapes and provides the theoretical basis for identifying the most critical excitation conditions. However, when oscillation amplitudes become large, the phenomenon becomes strongly nonlinear and may involve wave steepening, breaking, dissipation, and fluid-structure interaction effects that cannot be captured by linear theory alone. In such cases, CFD approaches are required to reproduce the transient evolution of the free surface and the associated wall pressure field with sufficient fidelity.
In partially filled horizontal tanks subjected to ship motion, the dominant excitation is often associated with pitch or roll. In the case of pitch motion, namely rotation about the transverse axis of the tank, the dominant fluid response is longitudinal sloshing. The effective gravity field in a rotating reference frame may be expressed as a vector whose components depend on the instantaneous pitch angle [9]:

$$a = \begin{pmatrix} g_x \\ 0 \\ g_z \end{pmatrix} = \begin{pmatrix} g\,sin\,\theta \\ 0 \\ -g\,cos\,\theta \end{pmatrix} \qquad \textit{Equation 3}$$

where g is the gravitational acceleration and θ is the instantaneous pitch or roll angle. If the imposed pitch motion is harmonic,

$$\theta(t) = \theta_{max}\,sin(\omega t) \qquad \textit{Equation 4}$$

with $\theta_{\max}$ the angular amplitude and ω the forcing angular frequency, the longitudinal component of gravity acts as the main forcing term for sloshing. For small angular oscillations, typically below about 10°, the linear approximations $\sin(\theta) \approx \theta$ and $\cos(\theta) \approx 1$ can be adopted, yielding the equivalent horizontal acceleration

$$a_x(t) \approx g\theta_{max}\,sin(\omega t) \qquad \textit{Equation 5}$$

4. CFD model description

The numerical model developed in this work was designed to reproduce the sloshing dynamics of liquid hydrogen in a partially filled marine storage tank under harmonic pitch excitation. The investigated configuration is based on an experimental campaign aimed at assessing the influence of sloshing on the internal fluid motion of a reduced-scale tank representative of a Type-C liquid hydrogen storage system for maritime transport. Two filling levels were considered, namely 81% and 65%, with liquid hydrogen initially at atmospheric pressure and cryogenic temperature conditions. The tank operates at 1 bar and the liquid phase is initialized at 20 K.
The experimental vessel is a geometrically scaled model of a full-scale marine tank. A geometric scale factor equal to 12.5 was adopted, resulting in a reduced tank volume of 2.6 m³ representative of a 5000 m³ Type-C tank installed on board a liquid hydrogen carrier operating in the North Sea. The internal geometry of the reduced tank consists of a horizontal cylindrical body closed by 2:1 semi-elliptical endcap. The main dimensions are an internal diameter of 1.05 m, a total length of 3.2 m, and an effective cylindrical length of 2.675 m. These values were used to define both the computational geometry and the characteristic dimensions governing the sloshing response.
The imposed tank motion was derived from full-scale ship dynamics through Froude similarity, which is appropriate for gravity-dominated free-surface flows. By enforcing equality between the Froude number of the real system and that of the experimental model, the characteristic time scale of the reduced configuration is obtained as proportional to the square root of the length scale. Assuming a representative natural pitch period of 10 s for a 200 m ship, the corresponding period for the scaled tank is 2.83 s, which gives an excitation angular frequency of approximately 2.22 rad/s. A pitch amplitude of ±5° was selected as a representative

severe but realistic operating condition. Accordingly, the reference excitation imposed in the simulations corresponds to an angular amplitude of 0.0873 rad and an angular frequency of about 2.2 rad/s.
To verify the consistency between the imposed forcing and the intrinsic sloshing dynamics of the tank, the first natural longitudinal sloshing mode was estimated through linear wave theory. Since pitch excitation primarily induces longitudinal oscillations, the relevant characteristic dimension is the effective cylindrical length rather than the tank diameter. Under the assumption that the first mode corresponds to half a wavelength inside the cylindrical section, the wave number can be written as $k = \pi / L_{cyl}$. By considering a representative filling depth equal to the tank radius, the first natural sloshing frequency is estimated from the Airy dispersion relation as approximately 2.49 rad/s, corresponding to a natural period of about 2.52 s. Therefore, the selected excitation frequency is close to the first natural longitudinal mode, ensuring a near-resonant condition suitable for reproducing severe and conservative sloshing scenarios in a realistic marine environment.
In the CFD model, the tank motion was not reproduced through mesh motion or rigid-body rotation. Instead, the pitch oscillation was represented through an equivalent time-dependent body-force approach. For small pitch angles, the horizontal component of gravity can be linearized, and the excitation can be expressed as a sinusoidal acceleration along the longitudinal direction using Equation 5, which, for the selected operating condition, becomes:

$$a_x(t) = g \cdot 0.0873\, sin(2.2t)\, m/s^2 \sim 0.856\, sin(2.2t)\, m/s^2 \qquad \textit{Equation 6}$$

Meanwhile, the acceleration along the y-direction is, for simplicity, assumed equal to the gravitational acceleration, $g = 9.81\ m/s^2$. This formulation provides a simple and effective way to reproduce the sloshing-inducing forcing inside the tank while preserving the main physics of the problem, as reported in Figure 1

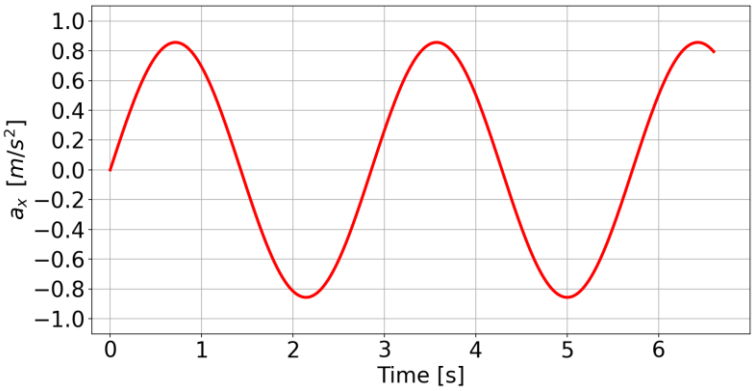

Figure 1. *Excitation expressed as a sinusoidal acceleration along the longitudinal direction of the tank*

Figure 2 qualitatively illustrates the relationship between the instantaneous angular position of the tank and the resulting longitudinal motion of the liquid. When the tank rotates clockwise, the liquid tends to accumulate on the right-hand side, whereas a counterclockwise rotation causes the liquid to shift toward the left-hand side. This behaviour can be explained by the projection of the gravity vector onto the tank longitudinal axis. In the tank-fixed reference frame, the longitudinal component of gravity acts as the driving force for the sloshing motion, and its sign depends on the instantaneous value of the rotation angle. Therefore, the liquid always tends to move toward the side of the tank that becomes lower during the oscillation.

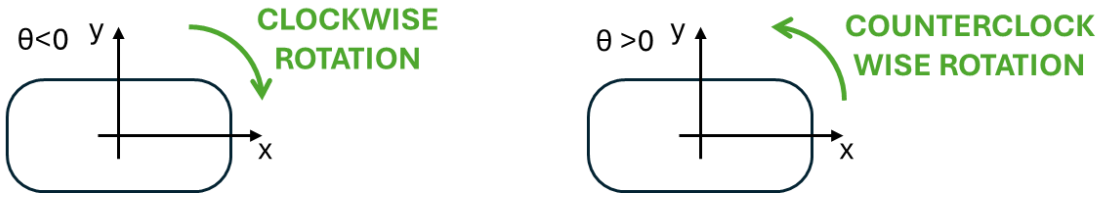

Figure 2. *Qualitative relationship between tank angular position and liquid redistribution during oscillatory motion*

In order to reduce the computational cost, only half of the tank was modelled by exploiting the geometrical symmetry of the system, resulting in a 180° domain. The resulting geometry includes the cylindrical section and the two semi-elliptical domes, with the liquid-gas interface initialized at the prescribed filling level. Two different numerical grids were generated, one for each filling ratio. The filling heights correspond to 850.5 mm and 682.5 mm for the 81% and 65% cases, respectively. A cutting plane located at the initial liquid level was used to separate the upper and lower tank regions before mesh generation (see Figure 3).
An unstructured tetrahedral mesh was adopted for both cases. The grid corresponding to the 81% filling level consists of about 0.5 million cells, while the grid for the 65% filling level includes about 1 million cells. In both meshes, local refinement was applied in the upper region of the tank and in the vicinity of the liquid-gas

interface, where the largest gradients of volume fraction and flow variables are expected. For the 81% filling case, the minimum cell spacing near the interface is approximately 15 mm, while the lower region of the tank is discretized more coarsely, with a maximum spacing of about 60 mm. Additional local refinement was introduced through a size-field strategy in selected critical regions, thus obtaining a suitable compromise between interface resolution and computational cost.

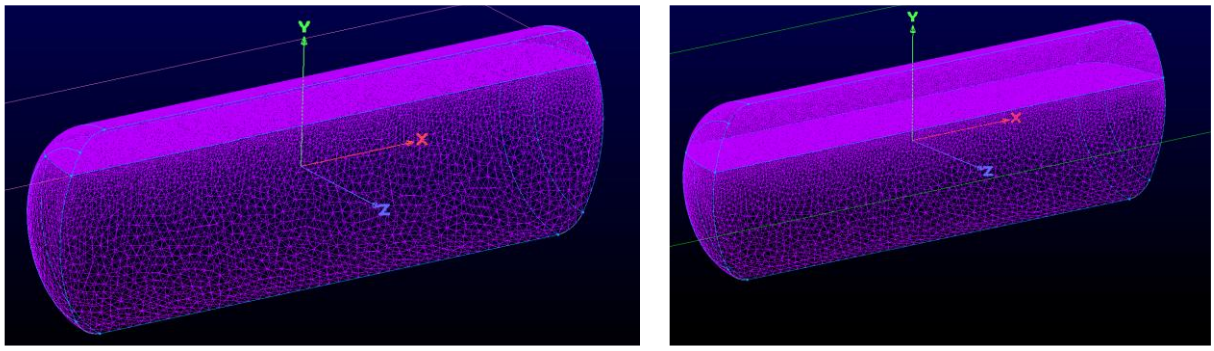

Figure 3. *Grid corresponding to the 81%and 65% filling level respectively, used for the CFD simulation*

The CFD model was implemented in ANSYS CFX [24] and solves the three-dimensional compressible conservation equations of mass, momentum, and energy within a homogeneous multiphase framework. In this approach, the liquid and gaseous phases share the same velocity, temperature, and turbulence fields, while the interface is tracked through the liquid volume fraction. The free surface between liquid hydrogen and gaseous hydrogen was modelled using the Volume of Fluid (VOF) method. Turbulence effects were described by means of the Shear Stress Transport (SST) turbulence model, which provides a robust balance between near-wall accuracy and stability in separated and transient flows. Since the present study is focused on pure sloshing dynamics, no mass transfer or phase change was included in the simulations.
Regarding material properties, gaseous hydrogen was modelled as an ideal gas, while liquid hydrogen was defined as a continuous fluid with constant saturation properties at 1 atm obtained from the REFPROP database. All solid boundaries corresponding to the tank wall were modelled as adiabatic no-slip walls, whereas the longitudinal cut plane was assigned a symmetry condition. Because the system is closed, no inlet or outlet boundaries were introduced. For buoyancy treatment, the reference density was set equal to that of the lighter phase, namely gaseous hydrogen, which is the recommended practice for free-surface simulations in ANSYS CFX [24].
The initial conditions were specified in terms of volume fraction, temperature, pressure, and velocity field. The liquid hydrogen volume fraction was set equal to unity below the prescribed filling level and zero above it, while the initial velocity field was set to zero throughout the domain. The liquid temperature was initialized at 20 K, consistent with the experimental condition, whereas the gaseous phase temperature was set to 22 K, slightly above the saturation temperature at 1 atm. The initial pressure field was imposed to ensure hydrostatic consistency in the liquid region and a uniform distribution in the gas region.
The transient simulations were performed using the high-resolution scheme for the discretization of convective terms and a second-order temporal discretization scheme. A time step of 10^{-3} s was selected in order to resolve the oscillatory motion of the free surface with sufficient temporal accuracy. The total simulated physical time was 30 s. Convergence within each time step was assessed through the root-mean-square residuals of the governing equations, with a target threshold below 10^{-4}. This setup was adopted for both filling levels to ensure a consistent comparison of the sloshing behaviour under the same excitation conditions

5. Results

This section presents the main results of the numerical simulations, with particular attention to the transient response of the liquid-gas system under oscillatory tank motion. The analysis focuses on the evolution of the main flow and thermodynamic variables in order to highlight the effect of sloshing on the internal behavior of the liquid hydrogen tank.
Figure 4 shows the time evolution of the absolute pressure inside the tank during the sloshing simulation. The pressure exhibits an overall decreasing trend over the entire simulated time, dropping from approximately 1.013 bar at the beginning of the transient to about 0.995 bar at t=30 s. Superimposed on this global pressure decay, small-amplitude periodic oscillations are observed, reflecting the dynamic response of the gas-liquid system to the imposed oscillatory motion. The periodic peaks are associated with the sloshing-induced redistribution of the liquid and the corresponding transient variation of the gas region. The progressive pressure decrease is likely related to the thermal interaction between the cold liquid hydrogen and the gaseous phase in the ullage region. Since the liquid is initially at cryogenic temperature, heat exchange from the gas toward the colder liquid can reduce the gas temperature during the transient. In a closed tank and in the absence of

mass addition, a reduction in gas temperature leads to a decrease in pressure, consistently with ideal gas behaviour. Therefore, the overall pressure decay can be reasonably interpreted as a consequence of gas cooling induced by the presence of the colder liquid phase. The small pressure fluctuations superimposed on the mean trend are instead associated with sloshing dynamics. As the liquid moves back and forth inside the tank, the shape of the free surface changes continuously, producing local compression and expansion of the gaseous region. This results in periodic pressure variations synchronized with the imposed excitation and the natural response of the fluid. Since phase change is neglected in the present simulations, the observed pressure decay cannot be attributed to evaporation or condensation effects. It is more likely related to the transient thermal equilibration between the liquid and gaseous phases, with the colder liquid hydrogen progressively cooling the ullage gas, possibly combined with the redistribution of the pressure field and an initial thermal adjustment of the system.

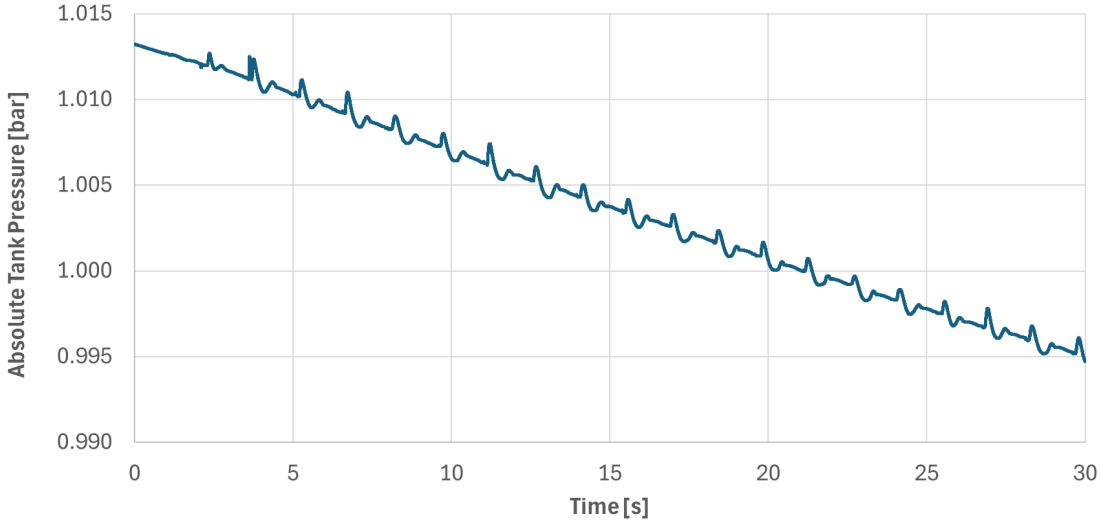

Figure 4. *Time evolution of the absolute pressure inside the tank during the sloshing simulation for the case at 81% filling level*

The pressure evolution shown in Figure 4 refers to the 81% filling level. A qualitatively similar trend was also observed for the 65% filling case, with an overall pressure decrease accompanied by small periodic oscillations associated with the imposed sloshing motion.

The sequence of volume-fraction contours highlights the strongly transient and nonlinear character of the sloshing motion at the 81% filling level. At the beginning of the simulation, the free surface remains relatively smooth and mainly follows the imposed tank oscillation, showing a moderate inclination consistent with the initial acceleration of the liquid mass. As time progresses, the wave amplitude increases and the free surface becomes increasingly asymmetric, indicating a progressive transfer of momentum from the tank motion to the liquid. Around $t = 2 - 3$ s the formation of a pronounced wave crest can be observed, together with the onset, of local overturning and partial breaking. This indicates that the sloshing response is no longer in a linear regime, but is dominated by strong inertial effects and by the interaction between the main travelling wave and the tank boundaries. The sequence also suggests a clear relationship between the imposed harmonic acceleration along the x-direction and the instantaneous position of the main wave inside the tank. Since the excitation is sinusoidal, the bulk liquid motion is alternately forced toward one end of the tank and then toward the other, and the wave crest tends to develop on the side toward which the liquid is being driven. However, this correspondence is not perfectly instantaneous. Owing to fluid inertia, wave propagation, and repeated wall interaction, a phase lag is expected between the external forcing and the free-surface response. This becomes particularly evident once the motion enters a strongly nonlinear regime, where run-up, local overturning, and recirculating structures progressively alter the simple sinusoidal response predicted by linear theory.

In the following stages, the liquid repeatedly impacts and runs up along the end caps, while the free surface undergoes large deformations and local fragmentation. The presence of steep fronts and recirculating structures suggests intense internal mixing and significant redistribution of the liquid volume inside the tank. The motion is therefore not limited to a simple oscillation of the interface, but involves complex three-dimensional flow features, including wave breaking, splashing, and repeated reversal of the dominant liquid motion from one side of the tank to the other. These features are consistent with a near-resonant sloshing condition, in which the imposed excitation frequency is close to the fundamental longitudinal mode of the tank.

Another important aspect is that the sloshing remains energetic even at later times. The snapshots at advanced stages of the simulation show that the interface does not relax toward a weakly perturbed condition, but instead maintains a highly deformed profile, with persistent run-up and overturning events. This suggests that the imposed oscillatory forcing continuously feeds the liquid motion, while dissipation is not sufficient to suppress the large-scale wave dynamics. Such behaviour is particularly relevant from an engineering perspective, since

it may lead to repeated local pressure loading on the tank walls, enhanced liquid-gas interaction, and stronger thermal mixing in the upper region of the tank.
Finally, the comparison between the early and late snapshots is also consistent with the pressure evolution discussed previously. While the mean tank pressure progressively decreases, the free surface continues to experience strong oscillations and local violent deformations. This confirms that the hydrodynamic response remains highly active throughout the transient, and that the observed pressure signal results from the combined action of global thermodynamic adjustment and local sloshing-induced oscillations.

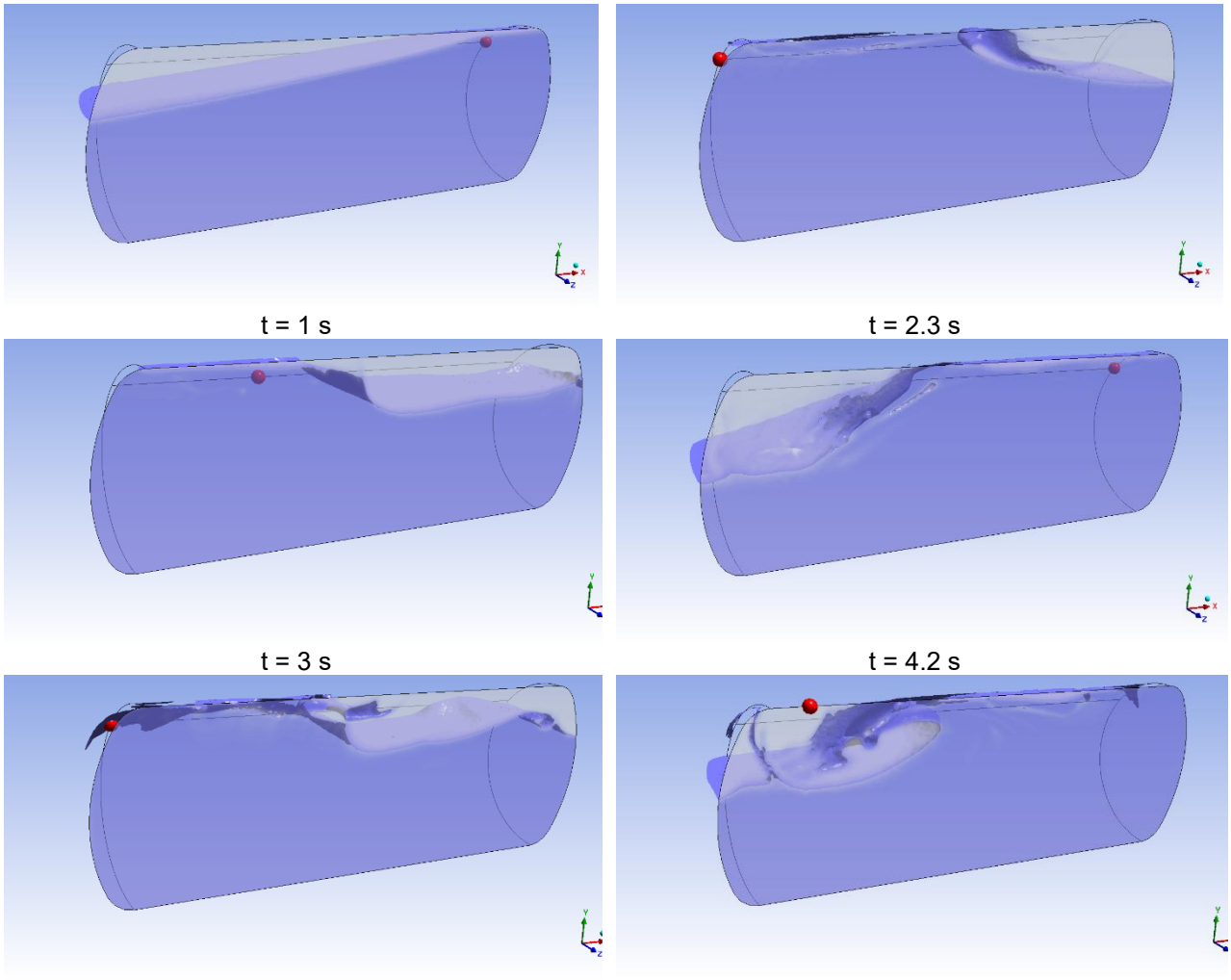

Figure 5. *Time sequence of liquid hydrogen free-surface evolution at 81% filling level during the sloshing simulation.*

Overall, the selected snapshots confirm that the imposed oscillatory motion induces a persistent and strongly nonlinear sloshing regime, characterized by large free-surface deformation, repeated run-up along the tank boundaries, and a phase-related but delayed response of the liquid with respect to the harmonic excitation.
In the selected snapshots reported in Figure 4, the red marker identifies the location of the maximum pressure on the upper wall of the tank at each considered time instant, thus providing a useful indication of the instantaneous redistribution of the pressure field within the ullage region. In the early stages of the motion, the marker appears to be located near the side reached by the incoming wave, suggesting a clear connection between the position of the pressure peak and the region where liquid run-up is most pronounced. As the wave approaches one end of the tank and rises along the wall, the gas volume above it is locally compressed, leading to an increase in pressure on the tank top in that area. As the oscillation develops, the position of the marker changes continuously, generally moving toward the side where the liquid accumulation and run-up are stronger. This behavior confirms that the pressure field along the tank top is highly non-uniform and is strongly affected by the instantaneous free-surface shape, as well as by the local interaction between the moving liquid and the gaseous phase.
Figure 6 shows the time sequence of the liquid hydrogen free-surface evolution at 65% filling level during the sloshing simulation. Compared with the higher filling condition, the lower liquid level allows a larger free-surface excursion and a more pronounced displacement of the liquid mass inside the tank. Starting from the initial configuration, the imposed oscillatory motion progressively amplifies the wave, which rapidly evolves into a

strongly nonlinear sloshing regime. The snapshots at intermediate times clearly show large-scale run-up along the tank walls, steep wave fronts, and marked asymmetry of the interface, indicating intense longitudinal liquid motion from one side of the tank to the other. As the oscillation develops, the wave crest undergoes overturning and local breaking, while the interface becomes increasingly distorted, suggesting enhanced internal mixing and stronger interaction between the liquid and gaseous regions. At later times, the free surface remains highly unsteady and does not return to a weakly perturbed configuration, confirming that the imposed excitation continuously sustains the sloshing motion. Overall, the figure indicates that the 65% filling level is associated with a highly energetic and strongly nonlinear sloshing response, characterized by significant liquid redistribution, repeated wall run-up, and persistent free-surface deformation throughout the simulation.
In comparison with the 81% filling case, the 65% configuration appears to promote a larger global displacement of the free surface, due to the greater available ullage volume and the larger space for wave development.

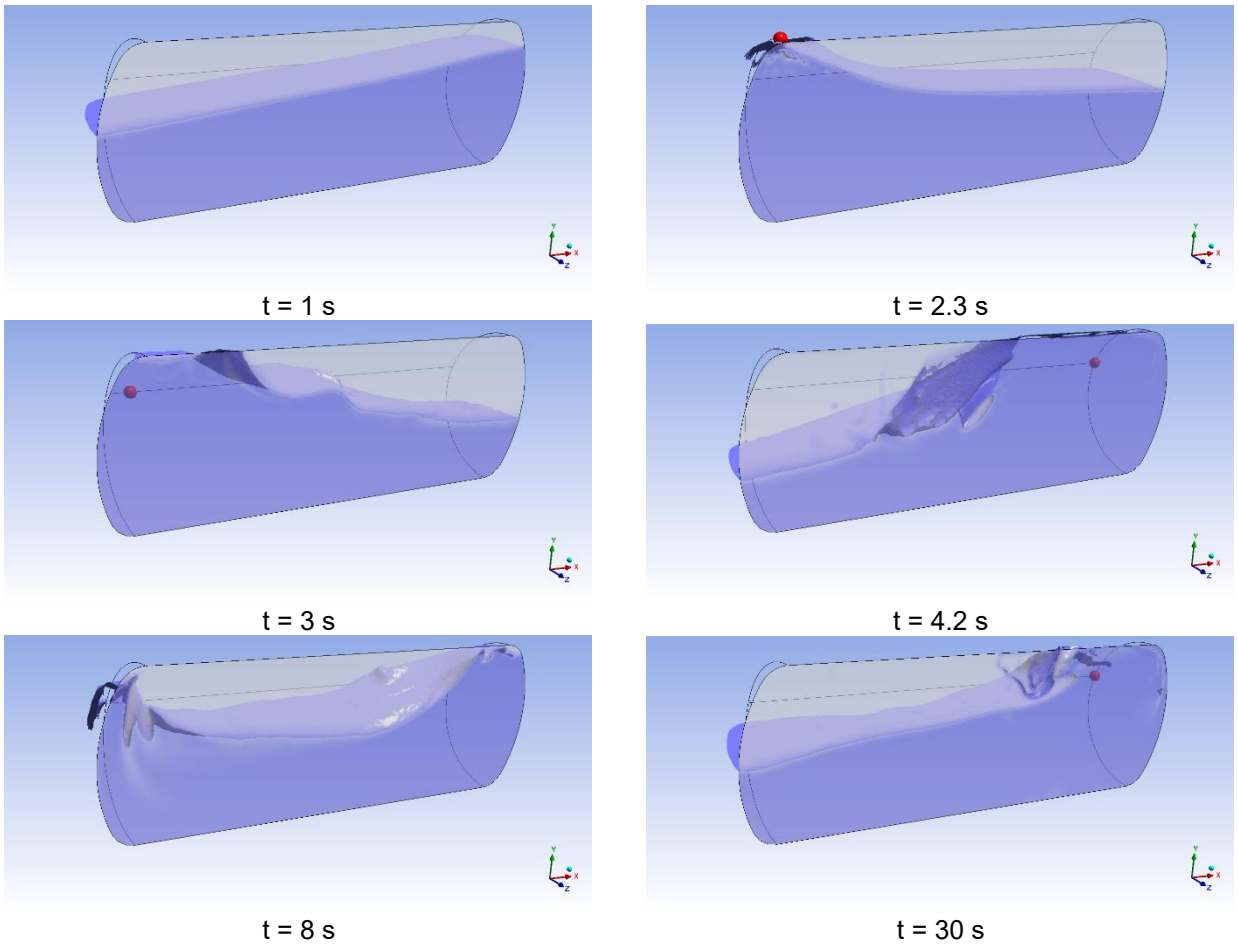

Figure 6. *Time sequence of liquid hydrogen free-surface evolution at 65% filling level during the sloshing simulation.*

Although the present results refer to a reduced-scale tank, they provide useful preliminary guidance for the corresponding full-scale LH_2 storage configuration, since the adopted scaling preserves the main gravity-driven sloshing dynamics. The observed wave amplification, repeated run-up along the end caps, and non-uniform pressure redistribution indicate that the upper wall and dome regions are likely to represent structurally critical areas under severe pitch-induced sloshing conditions. For the real tank, these zones should therefore be regarded as priority regions for local structural verification against transient loads, especially under operating conditions close to the fundamental sloshing mode. In this sense, the present results suggest that resonance avoidance, adequate shell stiffness, and, where necessary, local strengthening of the most exposed regions should be considered in the structural design process. However, these indications must be regarded as preliminary, since the present study does not include a dedicated structural assessment, fluid-structure interaction, or phase-change effects.

6. Conclusion

This work presented a CFD investigation of sloshing in a partially filled liquid hydrogen tank under oscillatory conditions representative of maritime transport applications. The study focused on the transient hydrodynamic

response of the liquid-gas system under harmonic excitation, with the aim of improving the understanding of free-surface evolution and pressure behaviour in cryogenic LH_2 storage tanks.
The results showed that, for both filling levels considered, the imposed oscillatory motion leads to a persistent and strongly nonlinear sloshing regime. In both configurations, the free surface rapidly departs from an initially smooth deformation and evolves into large-amplitude wave motion, with pronounced run-up along the tank walls and end caps, marked interface asymmetry, and local overturning phenomena. The selected snapshots also highlighted that the liquid response remains clearly phase-related to the imposed harmonic forcing, although the position of the main wave crest is not exactly synchronized with the excitation because of inertia, wave propagation, wall interaction, and nonlinear flow effects.
The pressure evolution inside the tank exhibited a common qualitative behaviour for the two filling levels, characterized by an overall decreasing trend with small periodic oscillations superimposed on the mean signal. The oscillatory component was associated with the cyclic compression and expansion of the ullage region induced by sloshing, while the mean pressure decay was interpreted as the result of transient thermal equilibration between the colder liquid hydrogen and the gaseous phase. Since phase change was not included in the present simulations, the pressure decrease cannot be attributed to evaporation or condensation effects, but rather to gas cooling, pressure redistribution, and initial thermal adjustment within the closed domain.
A comparison between the two filling conditions further confirmed the strong sensitivity of sloshing dynamics to the filling level. The 81% case showed severe sloshing with repeated run-up, large interface deformation, and significant local pressure redistribution near the tank top. At the same time, the 65% filling level appeared to promote an even larger global displacement of the liquid and more evident large-scale wave development, owing to the greater available free-surface extension and the larger ullage volume. In this case, the wave motion was characterized by more pronounced bulk liquid transfer from one side of the tank to the other, together with strong free-surface deformation and persistent nonlinear behaviour throughout the simulation.
The analysis of the free-surface evolution and of the pressure distribution also indicated that the upper wall and end-cap regions are likely to represent the most critical areas under severe sloshing conditions. In particular, the displacement of the maximum-pressure location on the tank top showed a clear dependence on the instantaneous wave position and on the local compression of the ullage caused by liquid run-up. Although the present simulations were performed on a reduced-scale configuration, the adopted similarity criteria allow the main gravity-driven sloshing features to be transferred qualitatively to the corresponding full-scale tank. From a structural standpoint, these results suggest that the dome and upper-wall regions should be considered priority areas for local verification under near-resonant operating conditions.
Overall, the present study confirms that CFD modelling is a useful tool for characterizing the sloshing dynamics of liquid hydrogen tanks and for identifying the main hydrodynamic features relevant to marine storage applications. Future work should extend the analysis toward a more complete thermo-fluid description, including phase change, thermal stratification, and boil-off, and should also address the coupling between CFD results and structural analyses in order to assess the full-scale response of LH_2 marine storage tanks under realistic operating conditions.

Acknowledgments

The authors would like to thank Gas and Heat S.p.A. for providing the design and operating data used as input for the CFD simulations carried out in this study

Nomenclature

CFD	Computational Fluid Dynamics
HHV	Higher Heating Value
LHV	Lower Heating Value
LH2	Liquid Hydrogen
SST	Shear Stress Transport
VOF	Volume of Fluid

References

[1] IEA (International Energy Agency). Net Zero by 2050 A Roadmap for the Global Energy Sector. 2021.
[2] Energy Agency I. World Energy Outlook 2024. 2024.
[3] International Renewable Energy Agency Abu Dhabi. GLOBAL energy transformation : A roadmap to 2050. IRENA; 2019.

[4] IEA (International Energy Agency). Global Hydrogen Review 2023. 2023. https://doi.org/10.1787/cb2635f6-en.
[5] Fuel Cells and Hydrogen Joint Undertaking (FCH). Hydrogen Roadmap Europe. 2019. https://doi.org/10.2843/249013.
[6] Redlich O, S Kwong JN. ON THE THERMODYNAMICS OF SOLUTIONS. V An Equation of State. Fugacities of Gaseous Solutions1. 2026.
[7] Soave G. Equilibrium constants from a modified Redkh-Kwong equation of state. vol. 27. Pergamon Press; 1972.
[8] FIuidMech J, Berg HJ, D RI, Co J, Sci I, K L V, et al. A New Two-Constant Equation of State. vol. 19. 1973.
[9] Grotle EL, Aesoy V. Numerical simulations of sloshing and the thermodynamic response due to mixing. Energies (Basel) 2017;10. https://doi.org/10.3390/en10091338.
[10] Raouf A. Ibrahim. Liquid Sloshing Dynamics Theory and Applications. Cambridge University Press; n.d.
[11] Hydrogen Safety for Energy Applications: Engineering Design, Risk Assessment, and Codes and Standards. 2022.
[12] R.D. McCarty, J. Hord HMR. Selected Properties of Hydrogen (Engineering Design Data). 1987.
[13] Rivkin C, Burgess R, Buttner W. Hydrogen Technologies Safety Guide. 2015.
[14] Aziz M. Liquid hydrogen: A review on liquefaction, storage, transportation, and safety. Energies (Basel) 2021;14. https://doi.org/10.3390/en14185917.
[15] Al Ghafri SZS, Swanger A, Jusko V, Siahvashi A, Perez F, Johns ML, et al. Modelling of Liquid Hydrogen Boil-Off. Energies (Basel) 2022;15. https://doi.org/10.3390/en15031149.
[16] Appel KR, Matveev KI, Leachman JW. Modeling the effects of liquid hydrogen tank operations on boil-off losses. Cryogenics (Guildf) 2025;150:104161. https://doi.org/10.1016/j.cryogenics.2025.104161.
[17] Barthelemy H, Weber M, Barbier F. Hydrogen storage: Recent improvements and industrial perspectives. Int J Hydrogen Energy 2017;42:7254–62. https://doi.org/10.1016/j.ijhydene.2016.03.178.
[18] Hossain Bhuiyan MM, Siddique Z. Hydrogen as an alternative fuel: A comprehensive review of challenges and opportunities in production, storage, and transportation. Int J Hydrogen Energy 2025;102:1026–44. https://doi.org/10.1016/J.IJHYDENE.2025.01.033.
[19] Langmi HW, Engelbrecht N, Modisha PM, Bessarabov D. Hydrogen storage. First Edit. Elsevier B.V.; 2021. https://doi.org/10.1016/B978-0-12-819424-9.00006-9.
[20] Makridis. Hydrogen storage and compression. Methane and Hydrogen for Energy Storage, 2016, p. 1–28. https://doi.org/10.1049/pbpo101e_ch1.
[21] Shin HK, Ha SK. A Review on the Cost Analysis of Hydrogen Gas Storage Tanks for Fuel Cell Vehicles. Energies (Basel) 2023;16. https://doi.org/10.3390/en16135233.
[22] Petitpas G, Benard P, Klebanoff LE, Xiao J, Aceves M. A Comparative Analysis of the Cryo-compression and Cryo-adsorption Hydrogen Storage Methods 2014.
[23] Faltinsen OM., Timokha AN. Sloshing. Cambridge University Press; 2009.
[24] ANSYS CFX 2025R1 User Manual 2025.